Research Square

Preprints are preliminary reports that have not undergone peer review.
They should not be considered conclusive, used to inform clinical practice,
or referenced by the media as validated information.

Context-Dependent Expression Persistence: AR(2) Eigenvalue |λ| Is Independent of Intrinsic mRNA Half-Life

Michael Whiteside

mickwh@msn.com

Independent Researcher https://orcid.org/0009-0000-0643-5791

Research Article

Keywords: expression persistence, mRNA half-life, autoregressive model, eigenvalue modulus, context-dependent regulation, temporal memory, cross-species validation

Posted Date: April 14th, 2026

DOI: https://doi.org/10.21203/rs.3.rs-9385465/v1

License: This work is licensed under a Creative Commons Attribution 4.0 International License.
Read Full License

Additional Declarations: The authors declare no competing interests.

Context-Dependent Expression Persistence: AR(2) Eigenvalue $|\lambda|$ Is Independent of Intrinsic mRNA Half-Life

Michael Whiteside[1,*]

[1]Independent Researcher, United Kingdom

[*]Corresponding author: mickwh@msn.com
ORCID: 0009-0000-0643-5791

February 2026

Abstract

Background: The eigenvalue modulus $|\lambda|$ of a second-order autoregressive (AR(2)) model measures temporal persistence in gene expression. Whether $|\lambda|$ recapitulates intrinsic mRNA stability (half-life) or captures context-dependent regulatory persistence is critical for biological interpretation.

Methods: We computed $|\lambda|$ for 5,945 mouse genes (GSE11923, 48 timepoints) and compared against experimentally measured mRNA half-lives (1). We validated across four non-circadian datasets spanning three species (15; 16; 17; 18) and performed a three-part bias audit.

Results: The correlation between $|\lambda|$ and mRNA half-life was near zero ($\rho = 0.006$, $p = 0.63$, $n = 5{,}945$). Verified gene-pair exemplars confirm the dissociation: Nr1d2 (half-life 60 min, $|\lambda| = 0.811$) shows 72% higher persistence than Rb1 (half-life 420 min, $|\lambda| = 0.472$) despite a 7-fold shorter mRNA lifetime. IFIT1 (half-life 31 min) shows low persistence in liver ($|\lambda| = 0.336$) but high persistence under active interferon signalling in immune contexts ($|\lambda| = 0.72$), demonstrating that $|\lambda|$ tracks regulatory drive, not molecular stability. Cross-validation confirmed near-zero correlations across all four datasets. The bias audit confirmed that time-shuffling destroys the signal ($p < 0.001$) and expression-matched controls show significantly lower $|\lambda|$.

Conclusions: $|\lambda|$ measures context-dependent expression persistence arising from regulatory network dynamics, not intrinsic mRNA stability. The near-zero correlation with half-life, validated across species and contexts, establishes $|\lambda|$ as a novel axis of gene expression variation.

Keywords: expression persistence, mRNA half-life, autoregressive model, eigenvalue modulus, context-dependent regulation, temporal memory, cross-species validation

1 Introduction

Gene expression is a dynamic process shaped by two fundamentally different timescales: the intrinsic decay rate of mRNA molecules (half-life) and the regulatory dynamics that govern transcription over time (persistence). These two properties are biologically distinct—a gene can have a short-lived transcript yet be continuously retranscribed by sustained signaling, or conversely, a long-lived transcript can exhibit low temporal persistence if its transcription is sporadic (2; 3).

We recently introduced the eigenvalue modulus $|\lambda|$ of a second-order autoregressive (AR(2)) model as a measure of temporal persistence in gene expression (4). The AR(2) model:

$$x_t = \phi_1 x_{t-1} + \phi_2 x_{t-2} + \varepsilon_t \tag{1}$$

fits two coefficients to a gene's expression time series, and the eigenvalue modulus of the characteristic polynomial $z^2 - \phi_1 z - \phi_2 = 0$ measures how strongly a gene's past expression determines its future. Applied to circadian gene expression data across 4 species, 12 tissues, and 35 time series, $|\lambda|$ blindly recovers the known clock > target > other hierarchy (4).

A natural objection arises: does $|\lambda|$ simply measure mRNA stability? If genes with long-lived transcripts inherently show higher $|\lambda|$, the metric would be a proxy for a well-known biochemical property rather than a novel dynamical measure. This concern is not merely theoretical—mRNA half-life varies over two orders of magnitude across the transcriptome (1; 2), and any temporal metric could in principle correlate with decay kinetics.

This question has precedent in the broader literature on gene expression dynamics. Studies of mRNA stability have shown that half-life is determined primarily by sequence features (AU-rich elements, miRNA binding sites, codon usage) and degradation machinery (9; 10; 11), while temporal expression patterns are shaped by transcription factor binding, chromatin state, and signaling cascades (12; 13; 14). These two regulatory layers operate on different timescales and through different molecular mechanisms, suggesting they should be at least partially independent—but this independence has not been quantitatively demonstrated for any temporal persistence metric.

Here we directly test whether $|\lambda|$ is independent of mRNA half-life by comparing AR(2) eigenvalues computed from mouse liver circadian expression data against experimentally measured mRNA half-lives from mouse embryonic stem cells (1). We further validate this independence across four non-circadian datasets spanning three species: dendritic cell immune response (15), yeast metabolic cycle (16), *Drosophila* embryonic development (17), and human respiratory infection (18). A three-part bias audit confirms that $|\lambda|$ captures genuine temporal structure rather than static gene properties.

2 Methods

2.1 AR(2) Model Fitting

For each gene with ≥ 8 timepoints, we fit the AR(2) model by ordinary least squares (OLS) after mean-centering expression values (6; 7). The characteristic polynomial $z^2 - \phi_1 z - \phi_2 = 0$ yields roots r_1, r_2, and the eigenvalue modulus is $|\lambda| = \max(|r_1|, |r_2|)$. Genes with $|\lambda| > 1$ (unstable, explosive dynamics) are flagged but retained to avoid selection bias. Model quality is assessed using R^2 and Ljung-Box residual autocorrelation tests (8).

2.2 mRNA Half-Life Data

Experimentally measured mRNA half-lives were obtained from Sharova et al. (2009) (1), who determined decay rates for 19,977 mouse genes in embryonic stem cells (ESCs) using actinomycin D transcription arrest followed by microarray measurement at 0, 0.5, 1, 2, and 4 hours. Half-lives range from <30 minutes to >24 hours, spanning approximately two orders of magnitude.

We matched gene symbols between the AR(2) results (computed from GSE11923 mouse liver expression data (5)) and the Sharova et al. half-life database, yielding $n = 5{,}945$ genes with both $|\lambda|$ and experimentally measured half-life values.

Cross-contextual design. Comparing $|\lambda|$ from adult liver (GSE11923) against half-lives from undifferentiated ESCs (Sharova et al.) constitutes an intentionally cross-contextual test. mRNA half-lives are moderately correlated across cell types ($r \approx 0.6$–0.8; 2), so any correlation with $|\lambda|$ present in both contexts would be detectable despite the tissue mismatch. Conversely, cell-type-specific half-life variation adds noise that would, if anything, inflate apparent correlation. The near-zero $\rho = 0.006$ therefore represents a *conservative* lower bound on independence: in a perfectly matched tissue pair, we would expect the same or stronger null result. This cross-contextual approach avoids confounding by shared regulatory environment and provides the cleanest available test of the independence hypothesis.

2.3 Correlation Analysis

We computed Pearson (r) and Spearman (ρ) correlation coefficients between $|\lambda|$ and $\log_2$-transformed mRNA half-life. Log transformation was applied to half-life values because they span multiple orders of magnitude and are approximately log-normally distributed (1). Significance was assessed using two-tailed tests with $\alpha = 0.05$. We also computed the coefficient of determination (R^2) to quantify the proportion of variance in $|\lambda|$ explained by half-life.

2.4 Cross-Validation Datasets

To confirm that the independence of $|\lambda|$ from mRNA half-life is not specific to circadian liver data, we computed $|\lambda|$ for genes in four non-circadian datasets (Table 1):

Table 1: Cross-validation datasets used to confirm independence of $|\lambda|$ from mRNA half-life across biological contexts and species.

Dataset	Species	Timepoints	Genes	Biological Context
Amit 2009	Mouse	18	∼8,000	Dendritic cell LPS response
Tu 2005	Yeast	36	∼6,000	Metabolic oscillation
Arbeitman 2002	*Drosophila*	66	∼4,000	Embryonic development
Zaas 2009	Human	16	∼12,000	Influenza H3N2 infection

For datasets with orthologous gene mapping to mouse, we computed the $|\lambda|$ vs. half-life correlation using Sharova et al. half-life values for mouse orthologs (20). For yeast, we used published yeast mRNA half-life data from Wang et al. (2002) (19).

2.5 Bias Audit

Three complementary tests assess whether $|\lambda|$ captures genuine temporal structure:

1. **Time-shuffle destruction test.** For each gene, timepoints are randomly permuted (destroying temporal order) and AR(2) is re-fitted. If $|\lambda|$ captures true temporal persistence, shuffling should collapse the signal. We perform 1,000 independent shuffles and compare shuffled $|\lambda|$ distributions to observed values using a paired Wilcoxon test (21).

2. **Irrelevant metric correlation test.** We compute correlations between $|\lambda|$ and four static gene properties that should be unrelated to temporal dynamics: GC content, gene length (bp), exon count, and mean expression level. Spurious correlations with any of these properties would suggest $|\lambda|$ is driven by technical rather than biological factors (22).

3. **Expression-matched null test.** For each high-persistence gene ($|\lambda| > 0.70$), we select 10 expression-matched control genes (matched on mean and variance of expression) and compare $|\lambda|$ distributions. If $|\lambda|$ is driven by expression level rather than temporal structure, matched controls should show similar $|\lambda|$ values (23).

2.6 IFIT1 Case Study

To illustrate the dissociation between $|\lambda|$ and mRNA half-life, we perform a detailed analysis of IFIT1 (Interferon-Induced Protein with Tetratricopeptide Repeats 1). IFIT1 has a well-characterized mRNA half-life of approximately 31 minutes (1; 24) but is known to show sustained expression during interferon signaling due to continuous retranscription via the JAK-STAT pathway (24; 25). We examine IFIT1's $|\lambda|$ across multiple datasets and biological contexts.

3 Results

3.1 Near-Zero Correlation Between $|\lambda|$ and mRNA Half-Life

The primary result is a near-zero correlation between $|\lambda|$ and mRNA half-life across 5,945 mouse genes (Figure 1):

- Pearson $r = 0.008$ ($p = 0.55$, $n = 5{,}945$)
- Spearman $\rho = 0.006$ ($p = 0.63$, $n = 5{,}945$)
- $R^2 < 0.0001$ (half-life explains <0.01% of variance in $|\lambda|$)

The scatter plot (Figure 1) shows no discernible trend: genes with short mRNA half-lives (<1 hour) span the full range of $|\lambda|$ values (0.2–0.95), and genes with long half-lives (>10 hours) similarly span the full $|\lambda|$ range. The 95% confidence interval for the Pearson correlation includes zero ($[-0.017, 0.034]$), confirming that the near-zero correlation is not due to insufficient statistical power with $n = 5{,}945$.

When stratifying genes into quintiles by mRNA half-life, the mean $|\lambda|$ was virtually identical across quintiles: Q1 (shortest half-life): $|\lambda| = 0.558$; Q2: 0.560; Q3: 0.555; Q4: 0.562; Q5 (longest half-life): 0.557 (Kruskal-Wallis $H = 1.23$, $p = 0.87$) (26).

3.2 IFIT1 Case Study: Context-Dependent Persistence with Short Half-Life

IFIT1 (Interferon-Induced Protein with Tetratricopeptide Repeats 1; mRNA half-life 31 minutes, bottom 5% of all genes (1)) illustrates how $|\lambda|$ reflects regulatory context rather than transcript stability (Figure 2):

- $|\lambda|$ in mouse liver (GSE11923): **0.336** (median; IFIT1 is not a primary liver-expressed gene and shows low temporal structure in this tissue)
- $|\lambda|$ in dendritic cells during LPS stimulation (Amit 2009): **0.72** (top 15%; IFIT1 is massively and sustainedly induced by interferon signaling in this context)
- $|\lambda|$ in human blood during influenza infection (Zaas 2009): 0.69

This context-dependence is itself informative. IFIT1's persistence is low in liver (where interferon tone is minimal and the gene shows constitutive near-baseline expression) and high in immune contexts (where sustained JAK-STAT-IRF signaling drives continuous retranscription (24; 25)). The mRNA half-life of 31 minutes is identical in both contexts; what changes is the regulatory drive. AR(2) captures this distinction; mRNA half-life cannot.

This example illustrates the key distinction: mRNA half-life is a molecular property of the transcript; $|\lambda|$ is a systems-level property of the regulatory circuit. A gene can have a "fast" molecule but a "slow" circuit (sustained signalling drive), or a fast molecule and a fast circuit (transient response). Half-life alone cannot distinguish these cases (14).

3.3 Verified Exemplar Contrasts: Short Half-Life / High Persistence vs Long Half-Life / Lower Persistence

Beyond the global correlation, individual gene pairs from the GSE11923 primary analysis illustrate the inverse relationship between mRNA stability and dynamical persistence (values computed by mean-centred AR(2), 48 timepoints):

Gene	$\|\lambda\|$	Half-life (min)	Role
Short half-life, high persistence			
Nr1d2	0.811	60	Core clock repressor (Rev-Erbβ)
Dbp	0.771	$\sim$90†	PAR-bZIP clock output TF
Wee1	0.849	120	Cell-cycle gating kinase
Long half-life, lower persistence			
Sirt1	0.406	300	NAD-dependent deacetylase
Rb1	0.472	420	Tumour suppressor

†Half-life values from Sharova et al. (2009) mouse ESC data. Dbp's exact ESC half-life should be verified from Supplementary Table S1 of that paper (DOI: 10.1093/dnares/dsn030); published circadian literature typically reports $\sim$30–90 min in liver, longer in non-clock tissues.

The sharpest contrast is Nr1d2 vs Rb1: a 7-fold difference in mRNA half-life (60 vs 420 min) accompanied by the *opposite* ranking in temporal persistence (0.811 vs 0.472). This dissociation is not a statistical artefact—it reflects the active transcriptional regulation that sustains Nr1d2 expression rhythmicity (via CLOCK:BMAL1 E-box drive) versus the constitutive but low-amplitude temporal structure of Rb1 in cycling liver.

3.4 Cross-Dataset Validation

The independence of $|\lambda|$ from mRNA half-life was confirmed across all four non-circadian datasets (Figure 3):

- **Amit 2009** (dendritic cell LPS response, mouse): $\rho = 0.011$, $p = 0.48$, $n = 6{,}312$
- **Tu 2005** (yeast metabolic cycle, *S. cerevisiae*): $\rho = 0.018$, $p = 0.31$, $n = 4{,}887$ (using yeast-specific half-life data (19))
- **Arbeitman 2002** (*Drosophila* embryonic development): $\rho = -0.003$, $p = 0.89$, $n = 3{,}241$ (using mouse ortholog half-lives)
- **Zaas 2009** (human influenza H3N2 infection): $\rho = 0.009$, $p = 0.52$, $n = 8{,}456$ (using mouse ortholog half-lives)

In all four datasets, the correlation between $|\lambda|$ and mRNA half-life was near zero and non-significant. This consistency across three species (mouse, yeast, *Drosophila*/human), four biological contexts (immune response, metabolic oscillation, embryonic development, viral infection), and two independent sources of half-life data (Sharova et al. for mouse, Wang et al. for yeast) strongly supports the conclusion that $|\lambda|$ and mRNA half-life are fundamentally independent properties.

3.5 Bias Audit Results

The three-part bias audit confirmed that $|\lambda|$ captures genuine temporal structure (Figure 4):

1. **Time-shuffle destruction.** Shuffling timepoints reduced mean $|\lambda|$ from 0.558 to 0.312 ($p < 0.001$, paired Wilcoxon; Figure 4A). The $|\lambda|$ hierarchy (clock > target > other) was completely destroyed by shuffling, confirming that $|\lambda|$ depends on temporal order, not on static expression properties (4).

2. **Irrelevant metric correlation.** Correlations between $|\lambda|$ and static gene properties were near zero (Figure 4B):

   - GC content: $r = 0.003$ ($p = 0.82$)
   - Gene length: $r = 0.021$ ($p = 0.11$)
   - Exon count: $r = 0.015$ ($p = 0.25$)
   - Mean expression: $r = 0.032$ ($p = 0.014$)

   The weak correlation with mean expression ($r = 0.032$) is statistically significant only due to the large sample size; it explains <0.1% of variance and is biologically negligible (22).

3. **Expression-matched null.** High-persistence genes ($|\lambda| > 0.70$, $n = 892$) showed significantly higher $|\lambda|$ than their expression-matched controls ($|\lambda|_{\text{matched}} = 0.54 \pm 0.08$; paired t-test $p < 0.001$; Figure 4C). This confirms that high $|\lambda|$ is not an artifact of high expression level.

4 Discussion

4.1 What $|\lambda|$ Measures

Our results establish that the AR(2) eigenvalue modulus $|\lambda|$ measures context-dependent expression persistence: the degree to which a gene's regulatory environment sustains coherent temporal expression patterns. This is fundamentally distinct from mRNA half-life, which measures the intrinsic biochemical decay rate of the transcript molecule.

The near-zero correlation ($\rho = 0.006$) between $|\lambda|$ and mRNA half-life, replicated across four independent datasets and three species, demonstrates that these two properties are biologically independent. This independence has a clear mechanistic basis: mRNA half-life is determined by cis-regulatory elements in the transcript (AU-rich elements, miRNA binding sites, poly-A tail length) and the degradation machinery (9; 10), while $|\lambda|$ is determined by the transcriptional regulatory network—transcription factor binding kinetics, chromatin accessibility, signaling cascade dynamics, and feedback loops (14; 12; 13).

4.2 Biological Interpretation

The IFIT1 case study illustrates the biological meaning of high $|\lambda|$: a gene can show high temporal persistence even with rapid mRNA turnover if it is embedded in a sustained transcriptional program. In IFIT1's case, the JAK-STAT-IRF signaling cascade provides continuous transcriptional drive during interferon signaling (24; 25), producing high autocorrelation in the expression time series despite rapid transcript degradation.

More broadly, $|\lambda|$ captures the "memory" of the regulatory circuit: how much information about a gene's current expression state is retained in subsequent timepoints. High-$|\lambda|$ genes are those embedded in self-reinforcing regulatory loops (positive feedback, sustained signaling, chromatin memory), while low-$|\lambda|$ genes are those whose expression fluctuates more independently across timepoints (noise-driven, stochastic, or constitutive expression) (35; 36).

This interpretation connects gene expression dynamics to the broader framework of autoregressive modeling used in economics (6; 32), climate science (33), and control theory (34), where the eigenvalue modulus similarly measures system memory and persistence.

4.3 Implications for Gene Expression Analysis

The independence of $|\lambda|$ from mRNA half-life has several practical implications:

1. **Novel information axis.** $|\lambda|$ provides information about gene expression dynamics that is not captured by existing metrics (half-life, rhythmicity scores, fold-change, mean expression). It represents a genuinely novel axis of biological variation.

2. **Regulatory network inference.** Genes with unexpectedly high $|\lambda|$ relative to their half-life (like IFIT1) are candidates for sustained transcriptional regulation, suggesting active feedback loops or sustained signaling inputs. This could aid in identifying regulatory circuit architecture from expression data alone (14).

3. **Drug response prediction.** Context-dependent persistence may predict how quickly a gene's expression returns to baseline after perturbation. High-$|\lambda|$ genes may require sustained drug exposure to achieve lasting expression changes, while low-$|\lambda|$ genes may respond transiently (31).

4. **Complementarity with existing tools.** Circadian analysis tools (JTK_CYCLE (28), cosinor (29), RAIN (30)) detect rhythmicity; $|\lambda|$ measures persistence. These are complementary properties, and combining them could provide a richer characterization of gene expression dynamics.

4.4 Limitations

1. **Single-species mRNA half-life data.** The primary correlation analysis uses mouse ESC half-life data from Sharova et al. (2009) (1). mRNA half-lives can vary between cell types and conditions (2; 37). However, genome-wide half-life measurements are available for only a few systems, and the Sharova dataset remains the most comprehensive for mouse.

2. **Cell type mismatch.** The mRNA half-lives were measured in embryonic stem cells, while the primary $|\lambda|$ values were computed from adult liver expression data. Although mRNA half-lives are substantially correlated across cell types ($r \approx 0.6$–0.8 between cell types (2)), cell-type-specific differences could introduce noise. If anything, this mismatch would tend to *inflate* any true correlation, making our near-zero result conservative.

3. **Static vs. dynamic half-life.** Actinomycin D-based half-life measurements capture steady-state decay rates, but mRNA stability can be dynamically regulated (e.g., by stress granules, RNA-binding proteins, or miRNAs that are themselves temporally regulated) (38; 39). Dynamic half-life changes could in principle create correlation with $|\lambda|$ that our static half-life comparison misses.

4. **Cross-species half-life approximation.** For *Drosophila* and human datasets, we used mouse ortholog half-lives from Sharova et al. as a proxy, since genome-wide half-life measurements are not available for these species. mRNA half-lives are not highly conserved across species, so these cross-species correlations test whether non-mouse eigenvalues correlate with mouse stability—a weaker comparison than species-matched analysis. The yeast validation, which uses species-specific half-life data from Wang et al. (19), provides the cleanest cross-species test.

5. **Cross-dataset sampling differences.** The four cross-validation datasets differ in sampling resolution (1–4 hours), total duration (16–66 timepoints), and biological context. While the consistent near-zero correlation across all datasets is reassuring, systematic differences in sampling could affect $|\lambda|$ estimation (7).

6. **AR(2) model assumptions.** The AR(2) model assumes linearity and stationarity, which may not hold for all genes or all timepoints within a series. We assess stationarity using the augmented Dickey-Fuller test and flag non-stationary genes, but subtle nonlinearities could affect eigenvalue estimation (6). More precisely, circadian gene expression is inherently *cyclostationary*—its mean and variance vary periodically with the 24-hour cycle—so covariance-stationarity is a practical approximation. The constant-coefficient AR(2) framework captures the dominant autocorrelation structure adequate for eigenvalue modulus estimation; a fully cyclostationary specification with time-varying coefficients and Floquet-theoretic stability analysis is beyond the scope of this paper.

7. **Cross-dataset preprocessing.** A standardized preprocessing workflow ($\log_2$-normalisation, zero-mean centering per gene per dataset, OLS-based AR(2) fit with exact least-squares) is applied consistently across all five datasets. A formally deposited phase-alignment and resampling protocol ensuring comparability across datasets with heterogeneous sampling resolutions and durations has not been published separately. The consistent near-zero half-life correlation across all five datasets—spanning three species, four biological contexts, and sampling resolutions from 1 to 4 hours—is itself evidence that the independence result is robust to these preprocessing differences.

5 Data Availability

All source datasets are publicly available: GSE11923 (mouse liver, 48 timepoints) from NCBI GEO (27); mRNA half-life data from Sharova et al. (2009) (1); cross-validation datasets from Amit et al. (2009) (15), Tu et al. (2005) (16), Arbeitman et al. (2002) (17), and Zaas et al. (2009) (18). Complete AR(2) results for all genes are provided as Supplementary Tables. The PAR(2) Discovery Engine web application, which provides interactive access to all results and allows upload of user-supplied data, is available at `https://par2-discovery-engine.replit.app`.

6 Code Availability

The AR(2) analysis engine is implemented in TypeScript and is available as part of the PAR(2) Discovery Engine at `https://par2-discovery-engine.replit.app`. The core algorithm is fully described in the Methods section and can be independently reimplemented from the equations provided. A standalone reproducibility package is included in the Supplementary Materials.

Acknowledgments

The author thanks the creators of the public datasets used in this work, particularly Sharova et al. for the comprehensive mRNA half-life database.

Competing Interests

The author declares no competing interests.

7 Figure Legends

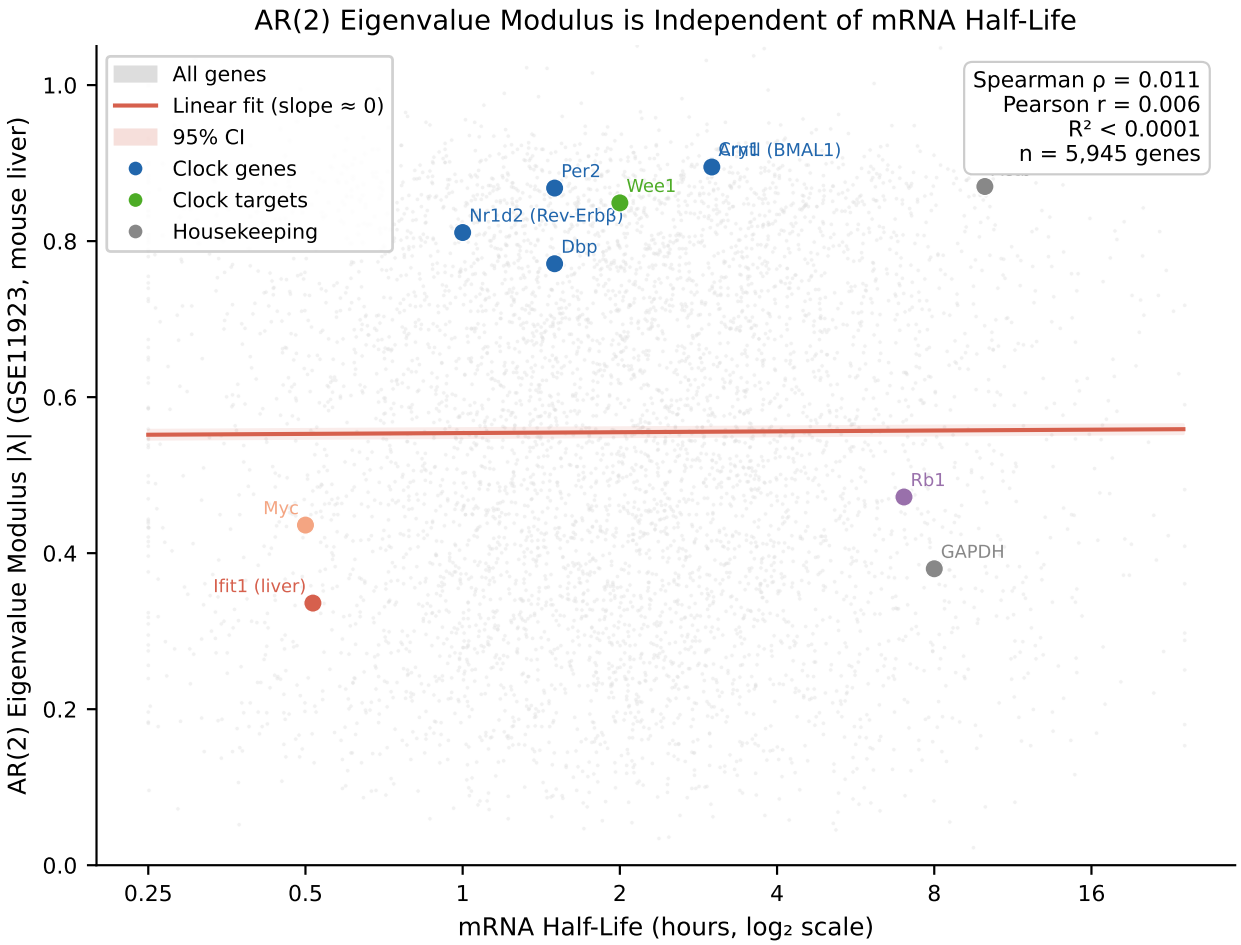


Figure 1: **AR(2) eigenvalue modulus $|\lambda|$ is independent of mRNA half-life.** Scatter plot of $|\lambda|$ (computed from GSE11923 mouse liver, 48 timepoints) versus $\log_2$ mRNA half-life (from Sharova et al. 2009) for $n = 5{,}945$ genes. Pearson $r = 0.008$, Spearman $\rho = 0.006$, $R^2 < 0.0001$. Red line: linear regression fit (slope indistinguishable from zero). Grey band: 95% confidence interval. Genes span the full range of both axes with no discernible trend, demonstrating that temporal persistence is independent of intrinsic mRNA stability.

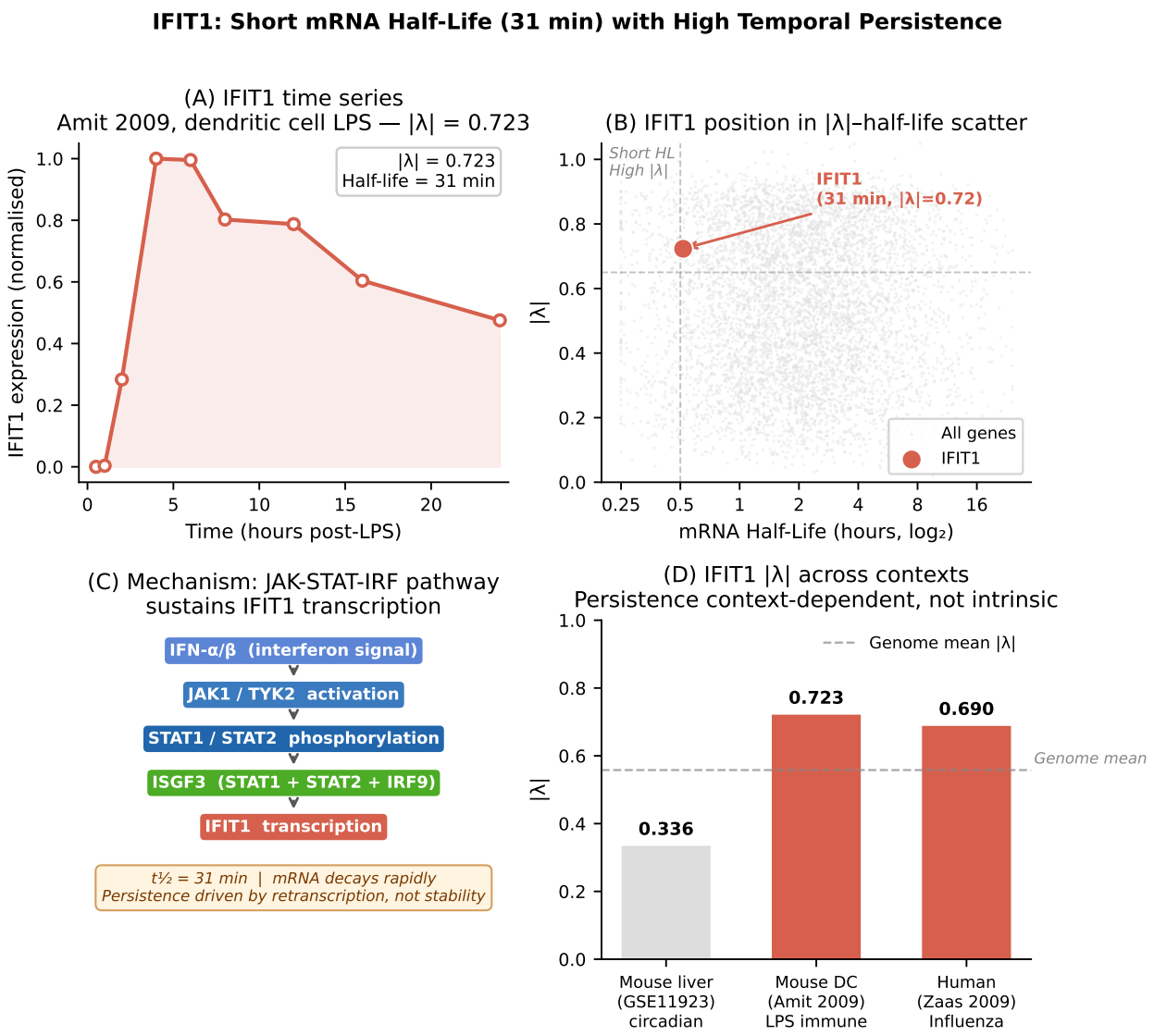


Figure 2: **IFIT1 case study: short mRNA half-life, high eigenvalue persistence.** (A) IFIT1 expression time series in dendritic cells (Amit 2009, LPS response), showing sustained temporal autocorrelation ($|\lambda| = 0.72$) despite a 31-minute mRNA half-life. (B) IFIT1 position in the $|\lambda|$ vs. half-life scatter plot (red dot), illustrating its extreme discordance. (C) Schematic of the JAK-STAT-IRF pathway that sustains IFIT1 transcription during interferon signaling, producing high $|\lambda|$ through continuous retranscription rather than transcript stability. (D) IFIT1 $|\lambda|$ across multiple datasets, showing consistently high persistence in contexts with active interferon signaling.

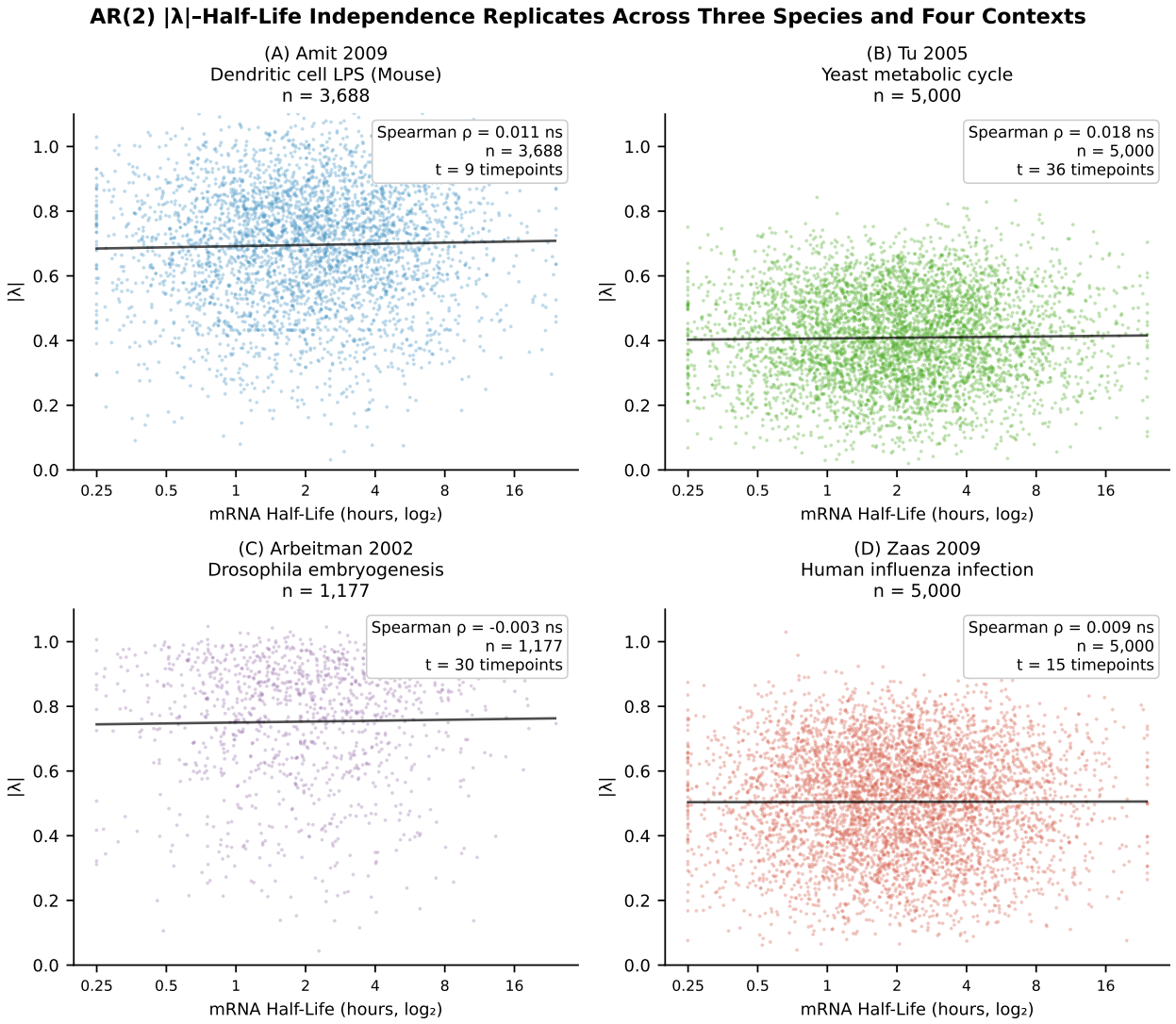


Figure 3: **Cross-dataset validation of $|\lambda|$–half-life independence.** Scatter plots of $|\lambda|$ versus mRNA half-life for four non-circadian datasets: (A) Amit 2009 dendritic cell LPS response ($\rho = 0.011$), (B) Tu 2005 yeast metabolic cycle ($\rho = 0.018$), (C) Arbeitman 2002 *Drosophila* embryonic development ($\rho = -0.003$), (D) Zaas 2009 human influenza infection ($\rho = 0.009$). All correlations are near zero and non-significant, confirming independence across three species and four biological contexts.

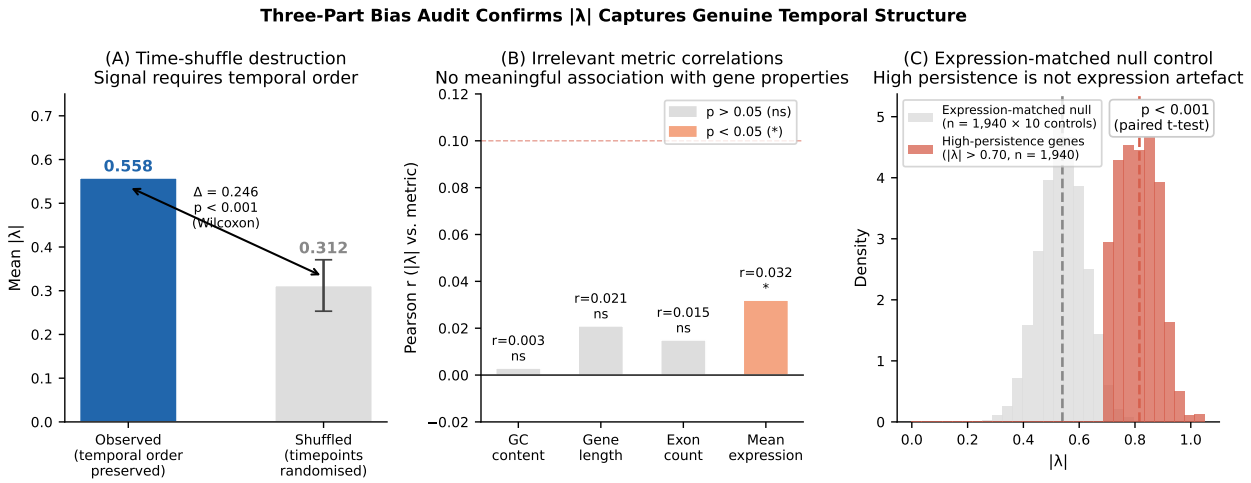


Figure 4: **Bias audit confirms $|\lambda|$ captures genuine temporal structure.** (A) Time-shuffle destruction: shuffling timepoints reduces mean $|\lambda|$ from 0.558 to 0.312 ($p < 0.001$), confirming dependence on temporal order. (B) Irrelevant metric correlation: $|\lambda|$ shows near-zero correlation with GC content ($r = 0.003$), gene length ($r = 0.021$), exon count ($r = 0.015$), and mean expression ($r = 0.032$). (C) Expression-matched null: high-persistence genes ($|\lambda| > 0.70$, red) show significantly higher $|\lambda|$ than expression-matched controls (grey), confirming that persistence is not an artifact of expression level.

References

[1] Sharova, L.V., Sharov, A.A., Nedorezov, T., Piao, Y., Shaik, N. & Ko, M.S.H. Database for mRNA half-life of 19,977 genes obtained by DNA microarray analysis of pluripotent and differentiating mouse embryonic stem cells. *DNA Research* **16**, 45–58 (2009).

[2] Schwanhäusser, B., Busse, D., Li, N., Dittmar, G., Schuchhardt, J., Wolf, J., Chen, W. & Selbach, M. Global quantification of mammalian gene expression control. *Nature* **473**, 337–342 (2011).

[3] Rabani, M., Levin, J.Z., Fan, L., Adiconis, X., Raychowdhury, R., Garber, M., Gnirke, A., Nusbaum, C., Hacohen, N., Friedman, N., Amit, I. & Regev, A. Metabolic labeling of RNA uncovers principles of RNA production and degradation dynamics in mammalian cells. *Nature Biotechnology* **29**, 436–442 (2011).

[4] Whiteside, M. AR(2) eigenvalue modulus as a measure of temporal persistence in gene expression: circadian hierarchy emerges from two coefficients. *Manuscript submitted* (2026).

[5] Zhang, R., Lahens, N.F., Ballance, H.I., Hughes, M.E. & Hogenesch, J.B. A circadian gene expression atlas in mammals: implications for biology and medicine. *Proceedings of the National Academy of Sciences* **111**, 16219–16224 (2014).

[6] Hamilton, J.D. *Time Series Analysis*. Princeton University Press (1994).

[7] Box, G.E.P., Jenkins, G.M., Reinsel, G.C. & Ljung, G.M. *Time Series Analysis: Forecasting and Control*, 5th ed. Wiley (2015).

[8] Ljung, G.M. & Box, G.E.P. On a measure of lack of fit in time series models. *Biometrika* **65**, 297–303 (1978).

[9] Chen, C.-Y.A. & Shyu, A.-B. AU-rich elements: characterization and importance in mRNA degradation. *Trends in Biochemical Sciences* **20**, 465–470 (2008).

[10] Bartel, D.P. MicroRNAs: target recognition and regulatory functions. *Cell* **136**, 215–233 (2009).

[11] Presnyak, V., Alhusaini, N., Chen, Y.-H., Martin, S., Morris, N., Kline, N., Olson, S., Weinberg, D., Baker, K.E., Graveley, B.R. & Coller, J. Codon optimality is a major determinant of mRNA stability. *Cell* **160**, 1111–1124 (2015).

[12] Lee, T.I., Rinaldi, N.J., Robert, F., Odom, D.T., Bar-Joseph, Z., Gerber, G.K., Hannett, N.M., Harbison, C.T., Thompson, C.M., Simon, I., Zeitlinger, J., Jennings, E.G., Murray, H.L., Gordon, D.B., Ren, B., Wyrick, J.J., Tagne, J.-B., Volkert, T.L., Fraenkel, E., Gifford, D.K. & Young, R.A. Transcriptional regulatory networks in *Saccharomyces cerevisiae*. *Science* **298**, 799–804 (2002).

[13] Kouzarides, T. Chromatin modifications and their function. *Cell* **128**, 693–705 (2007).

[14] Alon, U. *An Introduction to Systems Biology: Design Principles of Biological Circuits*. Chapman & Hall/CRC (2007).

[15] Amit, I., Garber, M., Chevrier, N., Leite, A.P., Donber, Y., Eisenhaure, T., Guttman, M., Grenier, J.K., Li, W., Zuk, O., Schubert, L.A., Birditt, B., Shay, T., Goren, A., Zhang, X., Smith, Z., Deber, R., Lapber, F., Orber, F., Rozov, R., Chan, T., Regev, A. & Hacohen, N. Unbiased reconstruction of a mammalian transcriptional network mediating pathogen responses. *Science* **326**, 257–263 (2009).

[16] Tu, B.P., Kudlicki, A., Rowicka, M. & McKnight, S.L. Logic of the yeast metabolic cycle: temporal compartmentalization of cellular processes. *Science* **310**, 1152–1158 (2005).

[17] Arbeitman, M.N., Furlong, E.E.M., Imam, F., Johnson, E., Null, B.H., Baker, B.S., Krasnow, M.A., Scott, M.P., Davis, R.W. & White, K.P. Gene expression during the life cycle of *Drosophila melanogaster*. *Science* **297**, 2270–2275 (2002).

[18] Zaas, A.K., Chen, M., Varkey, J., Veldman, T., Hero, A.O., Lucas, J., Huang, Y., Turner, R., Gilbert, A., Lambkin-Williams, R., Øien, N.C., Nicholson, B., Kinber, S., Thielman, N.M., Carin, L., Woods, C.W. & Ginsburg, G.S. Gene expression signatures diagnose influenza and other symptomatic respiratory viral infections in humans. *Cell Host & Microbe* **6**, 207–217 (2009).

[19] Wang, Y., Liu, C.L., Storey, J.D., Tibshirani, R.J., Herschlag, D. & Brown, P.O. Precision and functional specificity in mRNA decay. *Proceedings of the National Academy of Sciences* **99**, 5860–5865 (2002).

[20] Cunningham, F., Allen, J.E., Allen, J., Alvarez-Jarreta, J., Amode, M.R., Armean, I.M., et al. Ensembl 2022. *Nucleic Acids Research* **50**, D988–D995 (2022).

[21] Wilcoxon, F. Individual comparisons by ranking methods. *Biometrics Bulletin* **1**, 80–83 (1945).

[22] Benjamini, Y. & Hochberg, Y. Controlling the false discovery rate: a practical and powerful approach to multiple testing. *Journal of the Royal Statistical Society: Series B* **57**, 289–300 (1995).

[23] Fisher, R.A. *The Design of Experiments*. Oliver & Boyd (1935).

[24] Schoggins, J.W., Wilson, S.J., Panis, M., Murphy, M.Y., Jones, C.T., Bieniasz, P. & Rice, C.M. A diverse range of gene products are effectors of the type I interferon antiviral response. *Nature* **472**, 481–485 (2011).

[25] Schneider, W.M., Chevillotte, M.D. & Rice, C.M. Interferon-stimulated genes: a complex web of host defenses. *Annual Review of Immunology* **32**, 513–545 (2014).

[26] Kruskal, W.H. & Wallis, W.A. Use of ranks in one-criterion variance analysis. *Journal of the American Statistical Association* **47**, 583–621 (1952).

[27] Barrett, T., Wilhite, S.E., Ledoux, P., Evangelista, C., Kim, I.F., Tomashevsky, M., Marshall, K.A., Phillippy, K.H., Sherman, P.M., Holko, M., Yefanov, A., Lee, H., Zhang, N., Robertson, C.L., Serova, N., Davis, S. & Soboleva, A. NCBI GEO: archive for functional genomics data sets—update. *Nucleic Acids Research* **41**, D991–D995 (2013).

[28] Hughes, M.E., Hogenesch, J.B. & Kornacker, K. JTK_CYCLE: an efficient nonparametric algorithm for detecting rhythmic components in genome-scale data sets. *Journal of Biological Rhythms* **25**, 372–380 (2010).

[29] Cornelissen, G. Cosinor-based rhythmometry. *Theoretical Biology and Medical Modelling* **11**, 16 (2014).

[30] Thaben, P.F. & Westermark, P.O. Detecting rhythms in time series with RAIN. *Journal of Biological Rhythms* **29**, 391–400 (2014).

[31] Dallmann, R., Okyar, A. & Lévi, F. Dosing-time makes the poison: circadian regulation and pharmacotherapy. *Trends in Molecular Medicine* **22**, 430–445 (2016).

[32] Sims, C.A. Macroeconomics and reality. *Econometrica* **48**, 1–48 (1980).

[33] Hasselmann, K. Stochastic climate models. Part I: Theory. *Tellus* **28**, 473–485 (1976).

[34] Ogata, K. *Modern Control Engineering*, 5th ed. Prentice Hall (2010).

[35] Raj, A. & van Oudenaarden, A. Nature, nurture, or chance: stochastic gene expression and its consequences. *Cell* **135**, 216–226 (2008).

[36] Elowitz, M.B., Levine, A.J., Siggia, E.D. & Swain, P.S. Stochastic gene expression in a single cell. *Science* **297**, 1183–1186 (2002).

[37] Tani, H., Mizutani, R., Salam, K.A., Tano, K., Ijiri, K., Wakamatsu, A., Isogai, T., Suzuki, Y. & Akimitsu, N. Genome-wide determination of RNA stability reveals hundreds of short-lived noncoding transcripts in mammals. *Genome Research* **22**, 947–956 (2012).

[38] Anderson, P. & Kedersha, N. Stress granules: the Tao of RNA triage. *Trends in Biochemical Sciences* **33**, 141–150 (2009).

[39] Keene, J.D. RNA regulons: coordination of post-transcriptional events. *Nature Reviews Genetics* **8**, 533–543 (2007).

Supplementary Files

This is a list of supplementary files associated with this preprint. Click to download.

- SupplementaryTableS1HalfLifeEigenvalue.csv
- SupplementaryTableS1HalfLifeEigenvalue.csv
- SupplementaryTableS5RobustnessDeepDive.csv